



Design optimization of hybrid steel/timber structures for minimal environmental impact and financial cost: A case study



D. Van Cauteren*, D. Ramon, J. Stroeckx, K. Allacker, M. Schevenels

Faculty of Engineering Science, Department of Architecture, Architectural Engineering, KU Leuven, Leuven, Belgium

ARTICLE INFO

Article history:

Received 12 July 2021

Revised 1 October 2021

Accepted 17 October 2021

Available online 24 October 2021

Keywords:

Life cycle assessment

Life cycle costing

Structural optimization

Multi-objective optimization

Sustainable construction

ABSTRACT

In the overall aim to build more sustainably, the energy performance of buildings has received a lot of attention in the past decade. In consequence, the embodied impact of buildings has become relatively more important. As the load-bearing structure is responsible for a large share of this embodied impact, it is important to design it in such a way that its environmental impact is as low as possible. Unfortunately, the best construction materials in terms of environmental impact are not necessarily the cheapest. Reducing the environmental impact of the design may therefore lead to a higher financial cost, which may exceed the available budget. In such cases, hybrid structures, consisting of two (or more) different materials, might offer a solution, as they allow the designer to finetune the trade-off between environmental impact and financial cost. In this paper, we present a method to determine the best design of hybrid steel/timber structures in terms of environmental impact within the limits of the available budget. The method is based on the solution of a multi-objective structural design optimization problem involving environmental life cycle assessment and life cycle costing. It is applied to two test cases: a statically determinate and a statically indeterminate truss structure. The structures are optimized for three different design scenarios and typical load cases. This results in a Pareto front in the environmental and financial life cycle cost spectrum, allowing the designer to select the most appropriate solution, given the available budget. The results show that, depending on the design conditions, hybrid steel/timber structures are in some cases Pareto-optimal.

© 2021 Elsevier B.V. All rights reserved.

1. Introduction

The demand for a sustainable way of designing and building is constantly increasing in our present society. In current practice, focus is often put on improving the energy performance of buildings [9,11,21]. However, and especially for buildings with good energy performance, the importance of embodied emissions is increasing [35]. It is estimated that structural components in buildings are responsible for half of the emissions related to building materials [45]. Particularly, steel, cement, and aluminium were found to contribute to a high extent [33]. Structural design optimization (numerical optimization of structures) can reduce the amount of building materials used on the one hand, and select appropriate materials for the different components of the building structure on the other hand.

From a structural engineering point of view, architectural considerations aside, the aim is to obtain a structure that satisfies

the relevant performance criteria at the lowest possible environmental impact and financial cost. As in building practice the budget is usually limited, the challenge lies in finding the structural configuration with the lowest environmental impact available within these budgetary constraints. However, because there exists a trade-off between the environmental impact and the financial cost of a structure, it is not possible to minimize for both using a single-objective optimization approach. In contrast, a multi-objective optimization approach allows to uncover the trade-off between both aspects, which could be a powerful decision-making tool in the design stage. In this paper, we propose a methodology to achieve this, based on a combination of multi-objective structural optimization and life cycle assessment. Two case studies are presented where numerical optimization techniques are used to analyze the trade-off between the life cycle environmental impact and the life cycle cost of a structure. The study focuses on the performance of hybrid truss structures in terms of this trade-off for different design scenarios. In each scenario, different design conditions are considered (such as e.g. additional fire safety measures), possibly resulting in different optimal structures.

* Corresponding author.

E-mail address: daan.vancauteran@kuleuven.be (D. Van Cauteren).

Traditionally, a structural system is centered around the use of one specific material. In the field of structural optimization, it is often implicitly assumed that optimizing the sections of suchlike structures for minimal environmental impact or financial cost is equivalent to the minimization of the weight of the structure. In a hybrid structure, a combination of multiple materials is used for the structural elements, and this assumption evidently no longer holds. For example, increasing the sections of elements consisting of low impact material can enable reducing the sections of elements consisting of a high impact material, possibly resulting in a higher weight but a lower overall environmental impact. Similarly, the total financial cost of a structure is not directly proportional to the weight. Likewise, the structural performance of different materials may depend on the loading (e.g. for tie-rods, steel may be better than wood because a slender steel rod will suffice, while struts are susceptible to buckling, resulting in a larger cross-sectional area, also in the case of steel). To tackle this problem, a multi-objective optimization approach, accounting both for environmental impact and financial cost may offer a solution.

The idea to treat the weight, cost, energy performance, and environmental impact of building materials, structures or buildings independently in a multi-objective optimization formulation is a methodology applied in the literature. Evins et al. [19] present a study for the optimal design of a large roof canopy, where the member spacing and the number of primary truss bays are optimized. The weight-cost trade-off for (hybrid) steel structures and joint designs was presented by Mela et al. [26,28]. The trade-off between energy performance and structural performance of long span buildings was studied through a multi-objective optimization approach by Brown et al. [9]. Similarly, the trade-off of the embodied energy and the cost of prestressed concrete slabs was analyzed by Alcalá et al. [3]. Examples of similar optimization cases exist on building level. Wang et al. [44] deploy a genetic algorithm to optimize building performance using both economic and environmental criteria. Mela and Tiainen et al. [27,41] expand this economic and environmental multi-objective problem formulation by including designer preference through the maximization of free area without columns. The project time, cost, and environmental impact of large civil engineering projects is optimized for a tunnel design by Chen et al. [29]. The effectiveness of different decarbonization strategies on the life cycle environmental impact and life cycle cost of residential buildings is analyzed by Conci et al. [12], using a Pareto-efficiency approach. Najjar et al. [31] deploy life cycle assessment and building information modeling (BIM) in order to improve the energy performance and cost of buildings. It is clear that innovative methods, such as e.g. life cycle assessment (LCA) [22,23], life cycle costing (LCC) [24], BIM, and mathematical optimization strategies, have been deployed to generate overviews of the trade-offs of alternative designs in order to facilitate the decision making process during the design stage. The study of hybrid steel/timber structures however has, to the best of the authors' knowledge, not been the subject of a multi-objective optimization approach, where the life cycle environmental impact and the life cycle cost are optimized.

Environmental impact and financial cost minimization of structures are two prominent objectives in the field of structural optimization. For example, Brütting et al. [10] minimize the weight, cut-off waste, and embodied energy of spanning structures. The embodied energy of reinforced concrete structures was optimized by Yeo et al. [48]. Mavrokapnidis et al. [25] focused on cost-optimized structural systems and analyzed the corresponding energy consumption of these systems. However, in contrast to these examples, most structural optimization problems in the literature focus on weight minimization, which only reduces the energy and carbon embodied in the material mass, assuming that the structure consists of a single material [11]. In contrast, life

cycle assessment (LCA) takes into account the entire life cycle of a structure, allowing for a more comprehensive representation of the potential environmental impact and/or financial cost, and for the use of multiple materials [11]. Some studies implemented LCA in a structural optimization context [18,21,38]. These studies however focus on environmental impact or financial cost separately, or only a single environmental impact indicator is assessed. In this study, a multi-objective structural optimization problem is formulated, where a range of environmental impact indicators is included in the LCA (similar to Brütting et al. [11]), to optimize for both the environmental life cycle impact and the financial life cycle cost.

In this paper two case studies of hybrid (steel/timber) truss structures are presented where environmental LCA and life cycle cost assessment (LCC) are combined into a structural multi-objective optimization problem, enabling the detailed analysis of the impact-cost trade-off by using a Pareto-efficiency approach.

This paper is organized as follows. In Section 2, the case studies are introduced. In Section 3, the LCA and LCC framework and the structural analysis are discussed. Section 4 addresses the detailed formulation of the optimization problems. In Section 5, the results of the case studies are shown, followed by a discussion in Section 6. Section 7 presents the conclusions of the study.

2. Case studies

Two case studies are presented where hybrid steel/timber truss structures are optimized for both environmental life cycle cost (E-LCC) and financial life cycle cost (LCC). The specific truss structures for both case studies are introduced in Section 2.1. In each case study, we consider different design scenarios (indoor environment, outdoor environment, ...). These design scenarios are presented in Section 2.2. For each case study and each design scenario, the optimal section type has to be determined for every truss member, as well as its dimensions. The available section types (solid wood, laminated wood, solid steel, ...) are defined in Section 2.3.

2.1. Truss structures

In both case studies a truss structure is considered. Case 1 consists of a (2D) one-story truss, inspired by the Leonhardt House (Philip Johnson) (Fig. 1). Case 2 concerns a more complex structure, based on the (2D) four-story Mundo-A office building (B-architecten) (Fig. 2). Both structures are connected to the environment through a pinned support and a roller support. The two cases are chosen deliberately because of the difference in degree of static indeterminacy. Case 1 is statically determinate, whereas case 2 is statically indeterminate (over-determined). This implies that the element forces of the bars in case 1 remain identical throughout the entire optimization process so only one structural analysis is needed. For case 2 however every design update requires a structural analysis, as the element forces are related to the (updated) sectional properties of the bars.

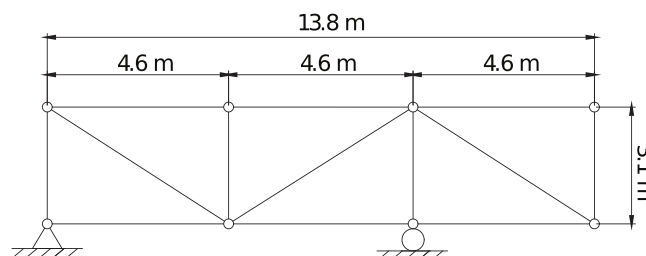


Fig. 1. Structural model for case study 1: statically determinate structure.

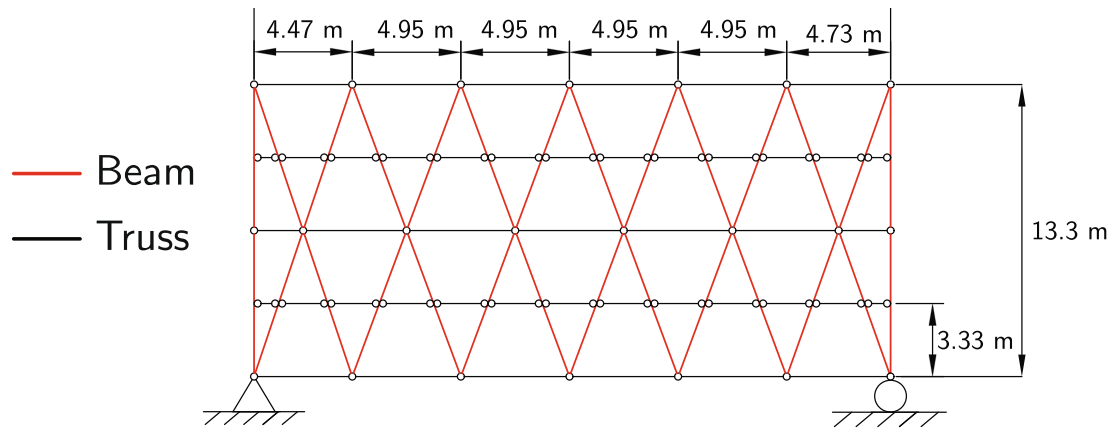


Fig. 2. Structural model for case study 2: statically indeterminate structure.

As shown in Fig. 2, the structure for case 2 is not strictly composed of bar elements. The diagonal members are modeled as Euler beams with pinned connections, allowing the transfer of shear forces and bending moments. This is a better representation of the original design; however, it adds complexity to the optimization problem.

2.2. Design scenarios

For each case study, the Pareto optimal designs are computed for three design scenarios. The scenarios represent different design conditions, which cause the need for additional treatments of the structural elements. The treatments come in the form of protecting layers, which impact the environmental impact and cost. Consequently, the optimal designs might differ for different scenarios.

In design scenario A, the structural elements are installed in a heated and climatized indoor environment. In design scenario B, the elements are subject to an outdoor environment. In design scenario C, the structures are installed in an indoor environment, but as part of a medium-sized or high-rise public building, which means that additional fire safety regulations have to be taken into account. This results in 6 individual cases, denoted as 1A, 1B, 1C, 2A, 2B, and 2C, where the number 1 or 2 refers to a truss structure and the letter A, B, or C refers to a design scenario.

2.3. Member sections

A selection of available timber and steel section types is made, based on engineering judgment. Table 1 shows the available section types for each case. The sections for scenario B are treated with wood preservation resins or anti-oxidation coating (steel), indicated by a blue border. Case study 1 classifies as a medium-rise structure and case study 2 as a high-rise structure. Therefore, the section types for case 1C comply with the European R60 standard and the section types for case 2C comply with the European R120 standard [47]. The timber sections are oversized by a fixed thickness and the steel sections are treated with fire-resistant paint, indicated by a red border. For the timber sections, different maintenance processes are defined based on the design conditions. Depending on the process a different frequency of the maintenance is needed (i.e. each 5, 10 or 20 years). A full life cycle inventory (LCI) of the member sections and their maintenance processes is included in Appendix A.

To manage the number of possible combinations of section types, a member grouping strategy is used. Figs. 3 and 4 show the different member groups in different colors for the 2 case structures. The groups imply that the same section type should

be used for every element of the same group. The dimensions of the sections may vary within the groups. Note that for non-diagonal member groups, the tie-rods are not included as a possible section type.

Table 1 shows that three fundamentally different section types can be distinguished. As presented in Fig. 5, the timber structural elements (hardwood and laminated girders) are modeled as solid rectangular sections. For the steel structural elements, two types of sections are used: (1) tubular rectangular sections and (2) solid circular sections for tie-rods. The dimensions indicated in Fig. 5 correspond to the design variables for each section and are bounded by the values in Table 2, based on commercial availability [8,30]. The design variables describe the dimensions of the base material. This implies that the oversizing amount (for fire protection) and the thickness of additional protecting layers is fixed (but the impact can still vary as the perimeter of the sections can change).

3. Simulation

In this section the structural analysis and the LCA and LCC framework are described. These simulations are integrated in the optimization in order to determine the objective function and/or constraints (Section 4).






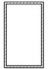






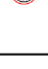
3.1. Structural analysis

The structures are modelled using the finite element method by means of the Matlab toolbox Stablib [20] as presented in Fig. 1 and 2, using bar and Euler beam elements. As case study 1 considers a statically determinate truss, a single finite element analysis at the start of the optimization loop suffices. For case study 2, where a statically indeterminate structure is considered, a finite element analysis is performed in every iteration of the optimization loop.

During the optimization, the structural performance requirements are safeguarded by monitoring the member forces (for buckling) and stresses for different load combinations. The structures are optimized for the load combinations displayed in Figs. 6 and 7 for truss structure 1 and 2, respectively. Linear elastic material behavior is assumed. The yield limit of the various materials is therefore used as maximum allowable value (Table 3). In case study 1, the sensitivities of the objective function and the constraints are computed analytically. In case study 2, the adjoint method is used, as the displacements are dependent on the design variables. The structural stability is verified through the implementation of an Euler buckling constraint. The serviceability limit state (SLS) was not included in the formulation of the optimization prob-

Table 1

List of available section types for each case study. The dots highlight the used section types in the specific case. Full LCI, with detailed descriptions is included in [Appendix A](#). A blue border denotes that treatments for an outdoor environment are applied, a red border indicates that fire-safety treatments are applied.

Section type	Description	1A	1B	1C	2A	2B	2C
	Hardwood section: indoor	●					
	Hardwood section: outdoor		●				
	Laminated girder: indoor				●		
	Laminated girder: outdoor					●	
	Oversized laminated girder: R60 fire resistant			●			
	Oversized laminated girder: R120 fire resistant						●
	Steel tubular section: indoor	●			●		
	Steel tubular section: outdoor		●			●	
	Steel tubular section: R60 fire resistant			●			
	Steel tubular section: R120 fire resistant						●
	Steel tie-rod section: indoor	●			●		
	Steel tie-rod section: outdoor		●			●	
	Steel tie-rod section: R60 fire resistant			●			
	Steel tie-rod section: R120 fire resistant						●

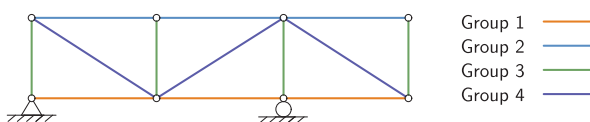


Fig. 3. Member groups for truss structure 1.

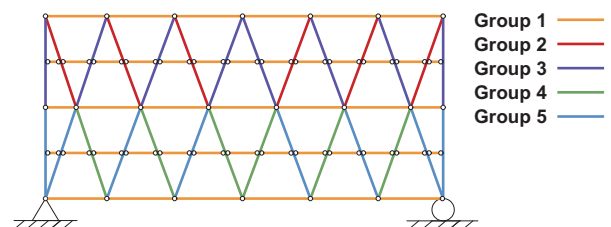


Fig. 4. Member groups for truss structure 2.

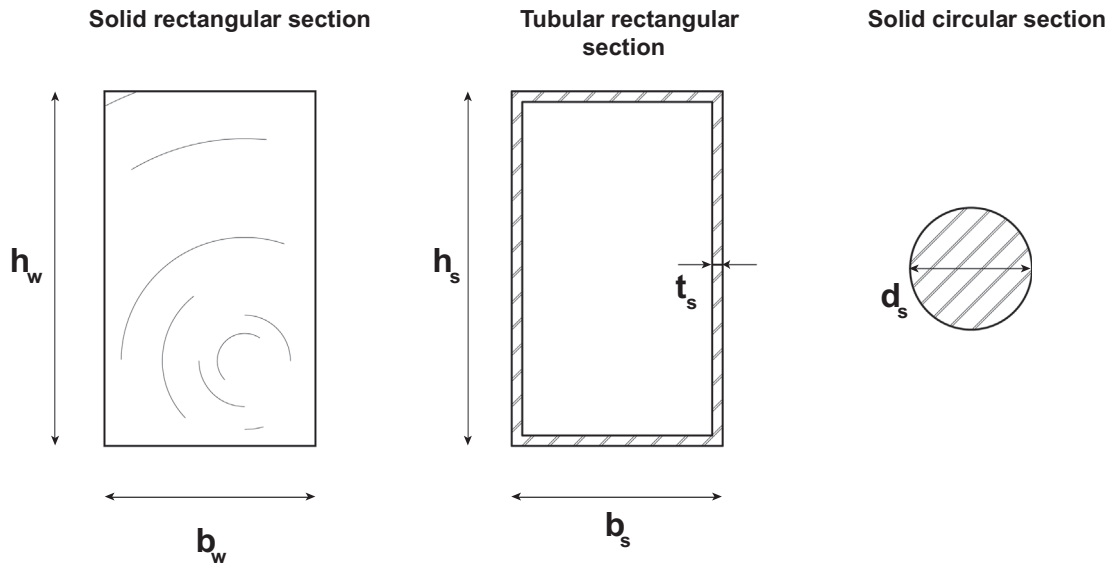


Fig. 5. The three section types used in the study and their corresponding dimensions: a solid rectangular section is used for the wooden elements (left), a tubular rectangular section (center) and a solid circular tie-rod section (right) are implemented for the steel sections.

Table 2
Lower and upper bounds for the design variables corresponding to the definition in Fig. 5.

	b_w	h_w	b_s	h_s	t_s	d_s
Lower bound [mm]	52	78	40	60	2	22
Upper bound [mm]	500	600	300	500	10	141

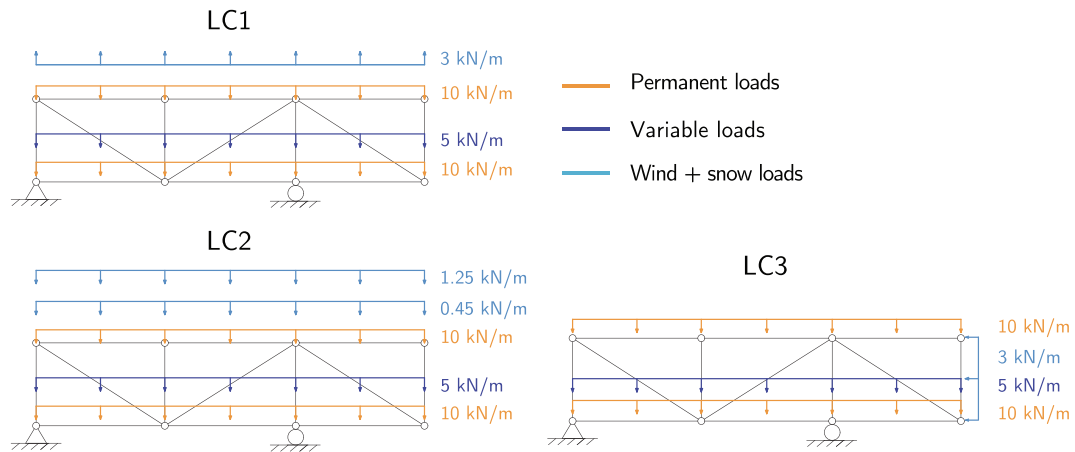


Fig. 6. Load combinations considered for case 1.

lem, but was checked afterwards and was satisfied for all optimized designs.

3.2. LCA framework

Within the framework of this paper, the MMG+ _KULeuven tool is used for the LCA and LCC calculations [42]. This tool uses the Belgian LCA method for buildings (Milieugelateerde Materiaalprestatie van Gebouwelementen (MMG) (Dutch) or Environmental profile of building elements (English) [6], described in this section) combined with a module for LCC calculations based on SuFiQuaD [4] (described in Section 3.3) in line with the ISO and European standards for LCA [22,23,16,15] and LCC [24,17].

3.2.1. Goal and scope definition

The goal of the study is to assess and minimize the life cycle environmental impact and life cycle cost of the two hybrid steel-timber truss structures, for the three different design scenarios.

It is assumed that the structural elements should at least have the same service life as the building. The Belgian LCA method for buildings (described in Section 3.2.2) assumes a reference service life of 60 years [6]. The average life expectancy of buildings is generally higher than 60 years, but it is assumed that after this period the building will be thoroughly renovated, implying that little of the original materials will remain. These renovations take place mainly in terms of functional and energetic improvements. Therefore the structure of the building remains intact most of the time.

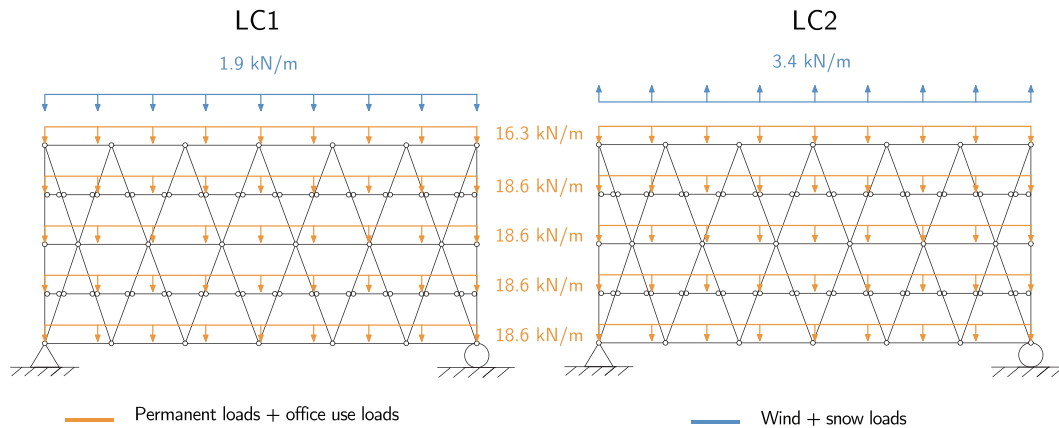


Fig. 7. Load combinations considered for case 2.

Table 3
Maximum allowable stress value for the different section types.

Section type	σ^{\max} [MPa]
Hardwood section	28
Laminated girder section	30
Steel tubular section	275
Tie-rod section	355

That is why in this study a higher service life of 80 years is considered for the structural elements, based on the average technical life of wood and steel beams [43]. This results in the definition of the functional unit as one meter of a structural element with an identical load-bearing capacity assuming a building service life of 80 years. This functional unit is the same for the LCC calculations described in Section 3.3.

3.2.2. Life cycle inventory and impact assessment

The Swiss life cycle inventory (LCI) database ‘Ecoinvent’ (Version 3.3) is used for gathering information on the in- and outputs of all the relevant processes during the service life of the structural elements [46]. The LCI data are harmonized to the Belgian context, by correcting electricity mixes and transport means in the datasets [6]. The LCI can be found in Appendix A.

The life cycle environmental impact assessment is performed according to the MMG method for building elements, i.e. the MMG (‘Environmental profile of building elements’) method [6]. The impact categories defined in the MMG method include the ones defined by the CEN TC350 standards [16,15]. These are further referred to as the CEN indicators. In addition, 10 more environmental indicators are included, referred to as CEN + indicators, at the request of the regional authorities in Belgium and are based on the International Reference Life Cycle Data System (ILCD) Handbook [14]. An overview of the impact categories is given in Table 4.

Within the MMG method, the 17 impact indicators are aggregated into a single score, expressed in monetary values (Euro) through a monetization step [34]. The monetization step is performed by multiplying the characteristic values (e.g. kg CO₂ eqv., kg CFC₁₁ eqv., etc.) (Table 5) with a monetary value per indicator. These monetary values express the cost of preventing the potential impact on the environment and/or estimate the possible damage caused by the emissions [6]. The obtained costs are hence external environmental costs, further referred to as E-LCC. Detailed information about the monetization method can be found in [13].

For the indicators ‘human toxicity’ and ‘ecotoxicity’, the data for these indicators has a high level of uncertainty. The LCA is per-

Table 4
Overview of the CEN and CEN+ impact indicators used in the MMG method [6].

CEN Indicators	CEN+ Indicators
Global warming	Human toxicity, cancer effects
Ozone depletion	Human toxicity, non-cancer effects
Acidification for soil and water	Particulate matter
Eutrophication	Ionising radiation, human health effects
Photochemical ozone creation	Ecotoxicity: freshwater
Depletion of abiotic resources: elements	Water resource depletion
Depletion of abiotic resources: fossil fuels	Land use occupation: soil organic matter
	Land use occupation: biodiversity
	Land use transformation: soil organic matter
	Land use transformation: biodiversity

formed mindful of the impact of these uncertainties. The designs are assessed, both including and neglecting toxicity effects, in order to acquire a full but nuanced analysis. For this study, the central values in Table 5 are used in line with the MMG method [13,6], so no sensitivity analysis is performed.

By totalling the cost to an aggregated score, the optimization problem (Section 4) can now be written in terms of a single objective function and or constraint.

The MMG+ _KULeuven tool calculates the E-LCC per meter for a bar. The total E-LCC $f_E(\mathbf{x}_d, \mathbf{x}_c)$ of a structure with n bars of length l , perimeter P , and area A in a configuration \mathbf{x}_d , is calculated as:

$$f_E(\mathbf{x}_d, \mathbf{x}_c) = \sum_{i=1}^n c_i l_i A_i(\mathbf{x}_d, \mathbf{x}_c) + d_i l_i P_i(\mathbf{x}_d, \mathbf{x}_c) \quad (1)$$

The constants c_i and d_i are acquired through the MMG + _KULeuven tool, and link the area and the perimeter of an individual bar to the E-LCC of that bar. They include the total of the monetized individual impact costs, associated with the area A and the perimeter P , respectively.

3.2.3. Considered life cycle phases and scenarios

Four life cycle phases are considered in the MMG method: production (A1-3), construction (A4-5), use (B1-7) and end-of life (EOL) (C1-4) (Fig. 8). In this study, all these phases are accounted for during the LCA. Module D covers the reuse and recycling phases, which is not yet included in the MMG method and consequently not considered within this study [6].

Life cycle scenarios have been defined for the transport, maintenance, replacement, and EOL processes occurring during the vari-

Table 5
Summary of the CEN+ environmental impact indicators considered in the LCA framework with their correlated unit, and monetization factors [34].

CEN+ impact indicator	Unit	Central monetization factor [€/unit]
Global warming	kg CO ₂ eqv.	0.05
Ozone depletion	kg CFC ₁₁ eqv.	49.1
Acidification for soil and water	kg SO ₂ eqv.	0.43
Eutrophication	kg (PO ₄) ₃ eqv.	20
Photochemical ozone creation	kg ethene eqv.	0.48
Depletion of abiotic resources: elements	kg Sb eqv.	1.56
Depletion of abiotic resources: fossil fuels	MJ, netcalorificvalue	0
Human toxicity: cancer effects	CTUh	665109
Human toxicity: non-cancer effects	CTUh	144081
Particulate Matter	kg PM _{2.5} eq	34
Ionising radiation: human health effects	kg U ₂₃₅ eq	9.7 × 10 ⁻⁴
Ecotoxicity: fresh water	CTUe	3.7 × 10 ⁻⁵
Water resource depletion	m ³ eq	0.067
Land use occupation: soil organic matter	kg C deficit	1.4 × 10 ⁻⁶
Land use occupation: biodiversity	m ² yr	
Urban		0.30
Agricultural		6.0 × 10 ⁻³
Forestry		2.2 × 10 ⁻⁴
Land use transformation: soil organic matter	kg C deficit	1.4 × 10 ⁻⁶
Land use transformation: biodiversity	m ²	
From urban land		N/A
From agricultural land		N/A
From forest		N/A
From tropical rainforest		27

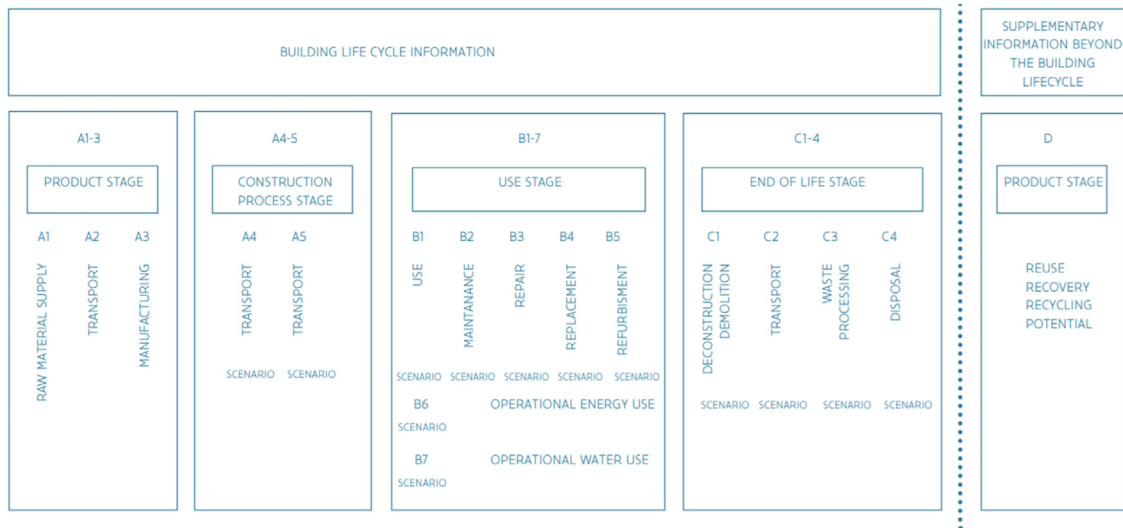


Fig. 8. Schematic overview of the considered life cycles phases in the MMG framework [6,15].

ous life cycle stages of the different elements and materials. These life cycle scenarios capture specific information regarding the quantity and frequency of events during the service life of the elements. The scenario for transport to the construction site is conform the standard scenario for prefabricated structural elements of the MMG framework [6]. The EOL scenarios are in line with the scenarios for metals and untreated, uncontaminated wood as predefined in the MMG method. The scenarios for maintenance were discussed in Section 2.2.

3.3. LCC framework

3.3.1. Basis of the framework

In order to uncover the trade-off between the environmental impact and the financial cost, the LCC of the structure is computed. The LCC method takes both initial investment costs and recurring

costs into consideration and aggregates them to obtain the life cycle financial cost. The costs that occur in the future are converted into present values and summed (i.e. sum of present values). Detailed information about the calculation of the present values can be found in [5]. Furthermore, the financial costs included in the assessment consider material, production, treatment, maintenance and EOL costs. Construction costs are neglected due to the lack of accurate data.

The MMG+ _KULeuven tool calculates the LCC per meter bar. The expression for the total LCC $f_c(\mathbf{x}_d, \mathbf{x}_c)$ of a structure with n bars of length l , perimeter P , and area A in a configuration \mathbf{x}_d , is formulated as:

$$f_c(\mathbf{x}_d, \mathbf{x}_c) = \sum_{i=1}^n g_i l_i A_i(\mathbf{x}_d, \mathbf{x}_c) + h_i l_i P_i(\mathbf{x}_d, \mathbf{x}_c) \quad (2)$$

Similarly as to Eq. (1), the constants g_i and h_i in Eq. (2) summarize the economic data associated with A and P .

3.3.2. Financial data

The cost data in the MMG+ _KULeuven tool are based on the SPON cost books for construction related products in the UK for the year 2015 [1,2]. The data are converted from pound to euro, using the currency exchange rate for 2015 of the European Central Bank (i.e. 1.38 €/£). The costs have moreover been updated to a nominal value for the year 2019 based on the I-index (i.e. 1.11), which reflects the evolution of the material prices in Belgium [7].

3.3.3. Economic parameters

The economic parameters during the service life of the structure are based on Belgian statistical data and correspond with the basic scenario defined in the SuFiQuad project [5]. An annual real discount rate of 2% and real growth rate for materials of 2% is assumed. Further a fixed VAT rate of 21% is assumed for all life cycle costs.

4. Multi-objective optimization

In this section, the optimization problem to determine the E-LCC and LCC Pareto front is formulated. In Section 4.1, the optimization problem is introduced. In Section 4.2, the solution strategy is described.

4.1. Formulation of the optimization problem

The multi-objective optimization problem consists of an inner (I) and an outer (II) problem. The design variables of the outer problem \mathbf{x}_d represent the section type for each bar based on the set \mathbf{X}_d of all possible section types defined in Section 2.3 (Table 1). The design variables of the inner problem \mathbf{x}_c represent the dimensions of the structural elements and are linked to the configuration of the different section types through the set $\mathbf{X}_c(\mathbf{x}_d)$ on which the box constraints are imposed implicitly (Table 2). The multi-objective problem minimizes for both the E-LCC (f_E) and the LCC (f_C). Additionally, the structural performance requirements $g_j(\mathbf{x}_d, \mathbf{x}_c)$ are imposed for the different load combinations.

$$\begin{aligned} & \underbrace{\min_{\mathbf{x}_d \in \mathbf{X}_d}}_{\text{II}} \underbrace{\min_{\mathbf{x}_c \in \mathbf{X}_c(\mathbf{x}_d)}}_{\text{I}} [f_E(\mathbf{x}_d, \mathbf{x}_c), f_C(\mathbf{x}_d, \mathbf{x}_c)] \\ & \text{s.t. } g_j(\mathbf{x}_d, \mathbf{x}_c) \leq 0 \quad j = 1, \dots, N \end{aligned} \quad (3)$$

The result of solving for the inner problem (I) is a curve which represents the Pareto front in terms of (f_E, f_C) for a fixed value of \mathbf{x}_d . Solving for the outer problem (II) results in a curve which represents the convex envelope of the curves in (I).

The objective functions f_E and f_C are computed using the LCA & LCC framework described in Section 3. Table 6 shows the dependence of A and P on the design variables \mathbf{x}_c . The analytical derivatives of the expressions in Table 6 are passed on as gradient information for the solver.

Table 6

Relation between the design variables \mathbf{x}_c (as defined in Fig. 5) and the perimeter P and the area A of the different section types.

	Rectangular section	Tubular section	Tie-rod
\mathbf{x}_c	b_w, h_w	b_s, h_s, t_s	d_s
P	$2(b_w + h_w)$	$4(b_s + h_s) - 8t_s$	πd_s
A	$b_w h_w$	$b_s h_s - (b_s - 2t_s)(h_s - 2t_s)$	$\frac{\pi d_s^2}{4}$

4.2. Solution strategy

The multi-objective optimization problem (3) is solved based on the distinction between the inner problem (I) and the outer problem (II). As mentioned, the inner problem results in a (f_E, f_C) Pareto front for a fixed configuration \mathbf{x}_d . The curve is obtained as the solution of a number of single-objective optimization problems, given by:

$$\begin{aligned} \text{(a)} \quad & \min_{\mathbf{x}_c \in \mathbf{X}_c(\mathbf{x}_d)} f_E(\mathbf{x}_d, \mathbf{x}_c) \\ & \text{s.t. } g_j(\mathbf{x}_d, \mathbf{x}_c) \leq 0 \\ \text{(b)} \quad & \min_{\mathbf{x}_c \in \mathbf{X}_c(\mathbf{x}_d)} f_C(\mathbf{x}_d, \mathbf{x}_c) \\ & \text{s.t. } g_j(\mathbf{x}_d, \mathbf{x}_c) \leq 0 \\ \text{(c)} \quad & \min_{\mathbf{x}_c \in \mathbf{X}_c(\mathbf{x}_d)} f_E(\mathbf{x}_d, \mathbf{x}_c) \\ & \text{s.t. } f_C(\mathbf{x}_d, \mathbf{x}_c) \leq f_C^k \\ & g_j(\mathbf{x}_d, \mathbf{x}_c) \leq 0 \end{aligned}$$

Sub-problems (a) and (b) are solved once, respectively minimizing the E-LCC and the LCC of the structure. Sub-problem (c) minimizes the E-LCC for a maximum allowable LCC f_C^k . This problem is solved for 6 (structure 1) or 4 (structure 2) equidistant values of f_C^k between the LCC values obtained for subproblems (a) and (b). This means that for every inner problem (I), 8 (structure 1) or 6 (structure 2) sub-optimizations are performed.

The inner problem (I) is solved using a gradient based algorithm. The gradient based solver used in this study is the method of moving asymptotes (MMA) for case 1 [39] and globally convergent MMA (GCMMA) for case 2 [40].

The outer problem (II) is solved by enumeration. The members are divided into member groups (Section 2.3), which impose that the same section type is used for the bars in the group (Figs. 3 and 4). This only reduces the number of configurations \mathbf{x}_d in \mathbf{X}_d ; the size of each bar is still optimized individually. For structure 1, 81 configurations are optimized. For structure 2, 72 configurations are optimized.

5. Results

5.1. Case 1: Statically determinate structure

In this subsection, the results for the statically determinate structure (cases 1A, 1B, and 1C) are presented. Fig. 9 shows the three cases as well as the E-LCC - LCC Pareto fronts for cases 1A, 1B and 1C and the corresponding convergence history of the Pareto optimal designs. Fig. 10 shows the environmental cost for the Pareto optimal designs grouped per environmental indicator.

Note that for most of the configurations, the eight resulting structures are within a very narrow range for both the E-LCC and LCC values, sometimes resulting in 8 identical designs (i.e. with the same member sizes). As the element forces are constant, the minimum required member sizes (to comply with the structural performance requirements) are the same for each configuration, resulting in only small E-LCC and LCC variations between different optimized designs with the same member section configuration.

Descending the Pareto fronts starting from the low E-LCC end, better steps are characterized by a steeper declining connection between two designs. As the Pareto fronts are convex, the efficiency of the steps always decreases with respect to the previous step. For all three scenarios, it can be seen that the Pareto optimal designs with more timber elements have a lower E-LCC but a

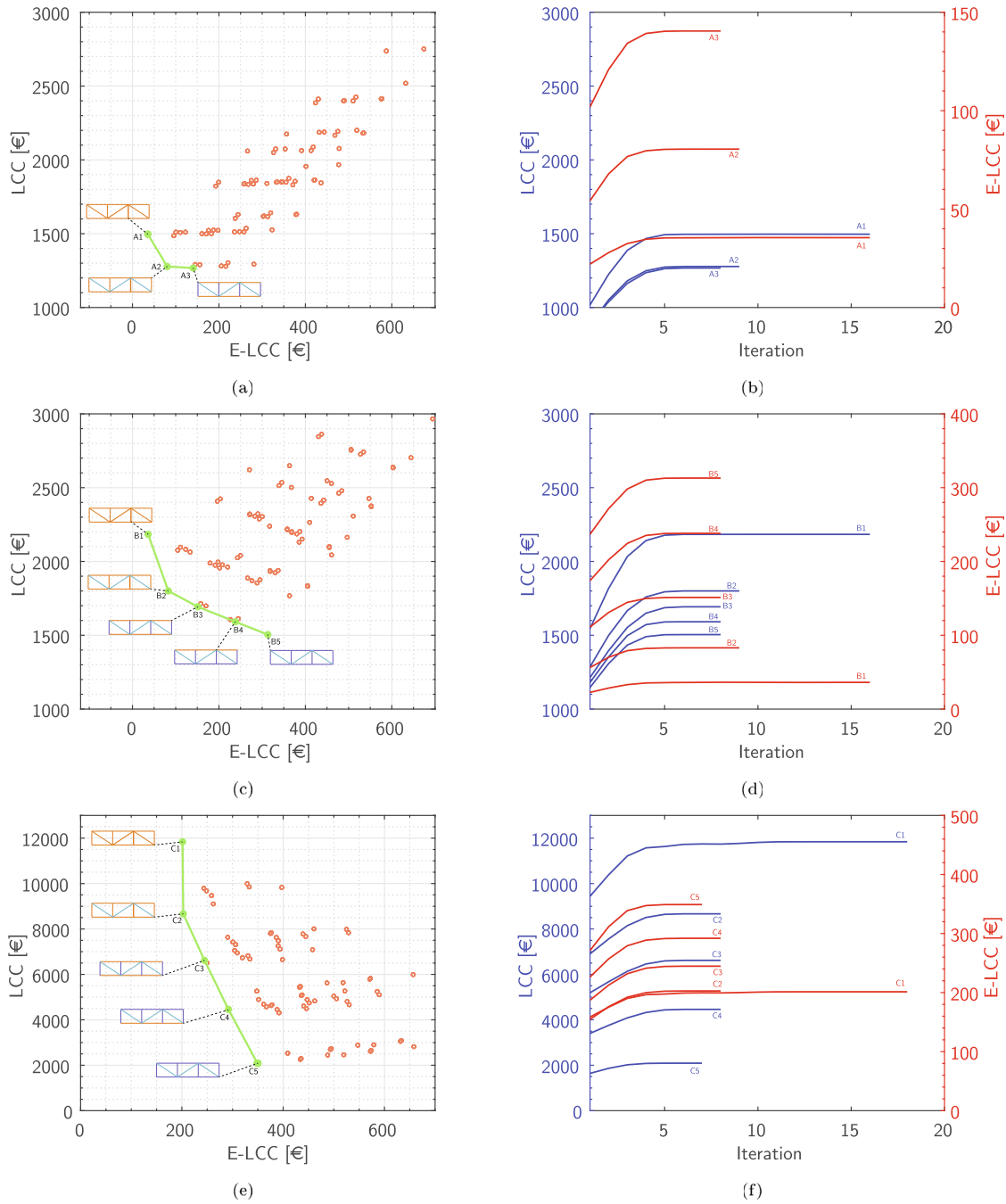


Fig. 9. E-LCC – LCC Pareto fronts for scenarios (a) 1A, (c) 1B and (e) 1C in Case 1. The front is highlighted in green, sub-optimal design are presented as red circles. The Pareto optimal structures are shown: the orange bars (timber section), dark blue bars (steel tubular section) and light blue bars (tie-rods) are scaled according to their cross section. The convergence history for the Pareto optimal structures is shown on the right for every design scenario.

higher LCC. For structures with more steel elements, the opposite is observed. In scenarios A and C, a hybrid design is optimal in terms of LCC and E-LCC respectively. Moreover, all intermediate Pareto optimal designs are hybrid steel-timber structures. This shows the relevance of the method used, as in practice the financial cost will always be limited by a fixed budget, in some scenarios not allowing to opt for the optimal E-LCC design.

For all scenarios, a timber structure with steel tie-rods on the diagonals performs well in terms of E-LCC. For scenario C, the difference with the optimal E-LCC design is negligible, yet the LCC is much lower, while for scenarios A and B, all-timber designs perform significantly better in terms of E-LCC. A possible explanation

for this could be the fact that the diagonals are always loaded in tension, implying that no buckling can occur, so small sections suffice. As scenario C simulates a fire resistant structure, the sections of the timber elements are oversized by a fixed thickness. This means that for smaller sections, the relative contribution of this thickness is larger, possibly resulting in a higher overall environmental impact than for the small tie-rod sections.

The Pareto fronts in Fig. 9 aid in making design decisions based on the available resources. For scenarios 1A and 1B, the LCC and E-LCC trade-offs between the single-objective optima lie within a different order of magnitude with respect to scenario 1C, indicated by the steepness of declination between the single-objective optima.

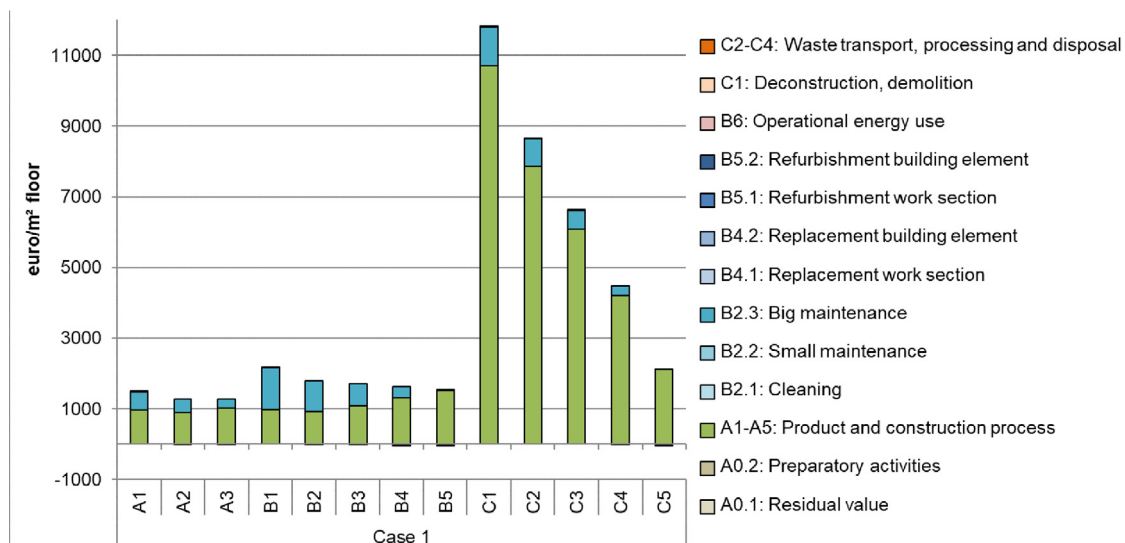


Fig. 10. Environmental cost for the different Pareto optimal structures grouped per environmental indicator for Case 1.

This means that in scenario 1C, a similar reduction of E-LCC requires a much larger investment in terms of LCC. A possible explanation for this phenomenon is the oversizing strategy, which makes timber members even more expensive in terms of LCC than they already are. The E-LCC - LCC trade-off between designs C1 and C2 is a good example of a situation where the reduced financial cost of the steel tie-rods (and the accompanying coatings) is much larger than the negligible decrease in terms of environmental impact, which is an effect that now is magnified due to the used oversizing strategy.

Analyzing the E-LCC results more in detail for the different Pareto optimal structures reveals that the production phase of the life cycle is responsible for on average 91–95% of the total environmental cost (Fig. B.1). The environmental impact linked to the Transport to site (A4) and Construction and installation (A5) together have a share of approximately 5%.

Regarding the contribution of the different environmental indicators to the overall environmental cost, steel elements are characterised by higher impacts for toxicity indicators as shown in Fig. 10, having an important contribution to the overall impact of the design. The toxicity indicators have a contribution of up to 63% for full steel designs (i.e. Pareto optimal structures B5 and C4), between 47% and 61% for designs containing steel elements, except for the Pareto optimal structure C1 where it is limited to 30%. Timber elements show lower values for all indicators with exception of land use occupation and biodiversity. For scenarios A and B, for timber designs (i.e. Pareto optimal structure A1, B1, and C1), the indicators ‘Land use: occupation, biodiversity’ and ‘Particulate matter’ are responsible for 60–63% of their total impact.

Considering the contribution of the different life cycle phases to the LCC results (see Fig. B.2), it is clear that for steel elements their overall cost is defined by the production cost, as maintenance costs are small. All-timber designs show a contribution of maintenance costs of 35% for A1, 55% for B1, and 9% for C1. For the hybrid designs, the maintenance costs vary between 21%–29%, 19%–49% and 6%–9% for respectively scenarios A, B and C.

In some cases it is obvious that, depending on the LCC budget, a clear choice can be made based on the set of intermediate Pareto optimal designs: e.g. for scenario A, the lowest LCC design only costs a fraction less for a huge additional E-LCC cost (4 times

higher); for scenario B, the step from a fully timber design to a timber design with tie-rod diagonals is the best improvement that can be made. Moreover, the results show that the choice for a specific configuration x_d has a large impact on the position in the E-LCC - LCC spectrum. In practice, the LCC and or E-LCC of different single material (or single section type) designs is compared to make design decisions. The optimizations show that hybrid designs should be included and that single material designs should not be an automatic choice, as most of the Pareto optimal designs (and in some scenarios the single-objective optima) are hybrid designs.

5.2. Case 2: Statically indeterminate structure

This subsection focuses on the statically indeterminate structure. Fig. 11 shows the E-LCC - LCC Pareto fronts for cases 2A, 2B, and 2C as well as the corresponding convergence history of the Pareto optimal designs. Notice the difference in spreading of the sub-optimal designs compared to case 1 (Fig. 9), as the six resulting designs for each configuration x_d now differ more distinctly. In some scenarios, the E-LCC score for sub-problem (c) (as described in Section 4.2) is lower than the E-LCC score for sub-problem (a), possibly caused by the fact that the additional constraint on the LCC score in (c) helps in bypassing the local optimum found in (a). This is not always the case, but important to keep in mind when interpreting the graphs.

The results show that the conclusions regarding case 1 are also applicable to case 2. All scenarios show that Pareto optimal structures with more timber elements tend to have a lower E-LCC, but a higher LCC. On the contrary, structures with more steel elements tend to be lower in LCC but higher in E-LCC. Again, all intermediate Pareto optimal designs are hybrid designs. Furthermore, all-timber designs with tie-rods on tension-loaded diagonals perform on the high end of the E-LCC scale and only perform slightly worse than a fully timber design (and in case 2C it even performs better). One can state that replacing tension loaded timber bars by steel tie-rods can be done based on engineering judgement during the design process, but the Pareto front also includes other less intuitive designs which probably would not have been considered without the use of a multi-objective optimization approach.

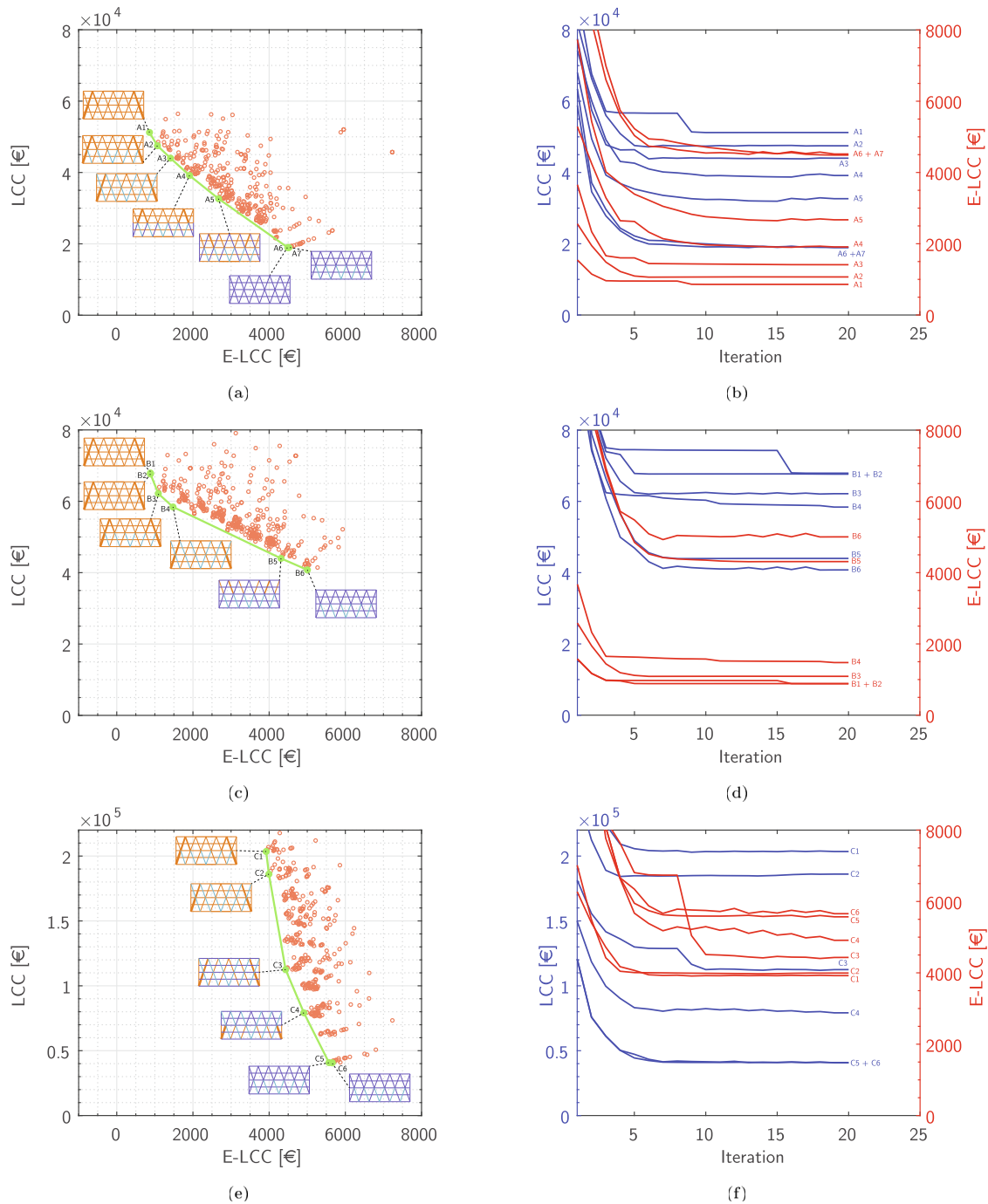


Fig. 11. E-LCC – LCC Pareto fronts for cases (a) 2A, (c) 2B and (e) 2C. The front is highlighted in green, sub-optimal design are presented as red circles. The Pareto optimal structures are shown: the orange bars (timber section), dark blue bars (steel tubular section) and light blue bars (tie-rods) are scaled according to their cross section. The convergence history for the Pareto optimal structures is shown on the right for every design scenario.

The Pareto front for scenario 2C again shows a steeper E-LCC – LCC trade-off compared to scenarios 2A and 2B. The smaller range on the E-LCC scale is caused by the higher environmental cost (almost double) of the oversized laminated girder compared to the hardwood section used in scenario A and the laminated girder in scenario B (see Fig. B.6). At the same time, the environmental cost of the steel tubular section and tie-rod section with a R120 fire resistance falls within the range of the sections used in scenarios A and B, resulting in a smaller range between the timber-steel design and the full steel design. The larger range on the LCC scale is caused by a similar mechanism. The cost of the steel design is

only slightly higher compared to scenarios A and B, while the cost of the oversized laminated girder used has almost doubled in comparison with the girders used in scenarios 2A and 2B, resulting in a much higher overall cost of the structure and causing a higher range.

Inspecting the E-LCC results of the Pareto optimal structures, the production phase is the most important (between 90% and 95%) life cycle phase (see Fig. B.4). The environmental impact linked to the Transport to site (A4) and Construction and installation (A5) have together a share of approximately 5%, Waste Disposal (phase C4) also has an impact of up to 3% when laminated

girders are used in the design. Its importance decreases with increasing steel use in the design.

Similarly as in case 1, the toxicity indicators have a high contribution to the overall environmental cost of the designs containing steel elements (see Fig. B.3). The difference in environmental cost between the Pareto optimal structures A4 and A5, A5 and A6, B4 and B5 are caused by a general increase of all indicators because of the higher amount of steel elements in the design, but in particular the impact for the toxicity indicators increased a lot to up to 62 % and 61 % for the structures A6 and B5. Further, similar trends such as a decrease in the importance of the 'Land use: occupation, biodiversity' and 'Particulate Matter' indicators with the decreasing amount of timber in the design is found here.

For the financial cost (see Fig. B.5), also maintenance has an important contribution to the total cost of scenario B, up to 43% for the Pareto optimal structure B6. For scenarios A and C, the maintenance cost is decreasing with a decreasing amount of timber elements in the design.

6. Discussion

It is clear that the toxicity indicators play an important role in the overall environmental cost of the optimized structures. Within the MMG methodology, the USEtox-method © by Rosenbaum et al. is used [36]. It is known that there are some important modelling gaps with metals in this model [32,37], which explains the high values for all toxicity indicators and increasing trend with an increasing amount of steel elements in the design. Therefore, the optimization runs were also performed excluding these toxicity indicators. In most cases, the Pareto optimal structures and by consequence the Pareto front did not change. Only for scenario C (for both cases), the Pareto front was reduced to one single point, being the structure C5 in Fig. 9 and C6 Fig. 11. When excluding the toxicity indicators in Fig. B.6, it can be seen that the environmental impact of the steel tubular section is only slightly higher than the one for the timber section for the R120 fire resistance scenario. For cases 2B and 2C, there is still a significant difference between the steel and timber sections resulting in the same Pareto optimal structures. In case of the fire safety design scenario, it is important to consider a holistic assessment approach to avoid a burden shifting.

It is important to note that the amount of configurations was reduced due to the introduction of member section groups. Even though these groups are selected based on engineering judgement, the design space is limited, meaning that different optimal designs could exist. In addition, the possible member section types are selected based on a preliminary study. The composition of the larger selection of member section types included in this study also relies on engineering judgement and experience.

This study considers the financial costs over the full service life of the structures studied. However, it should be noted that the costs related to the construction of the structures are not fully taken into account as they are also construction site specific. Nevertheless, based on information from architectural offices, it is not expected that this would lead to additional differences between the intermediate Pareto optimal structures. In addition, including the joint design in the life cycle assessment could impact the configurations of the Pareto optimal designs, but this was not taken into account in this paper. Further, the study includes a residual value for steel, but not for timber. As these residual values are limited for the steel elements, it only influences the final cost to a very limited extent. Nonetheless, in the idea of circular economy and reuse of the different sections in a later stage, further investigations about the residual value of these element and their influence on the total cost would be interesting.

7. Conclusion

Sustainable design and construction is getting increasingly more attention in current academic research but also in our present society. When focusing on the structural components of buildings, the importance of the embodied emissions is growing at a rapid pace. Therefore, there is a need to analyze and improve the way structures are designed with respect to their environmental impact across the complete life cycle of their components. Accordingly, the introduction of scientific methods such as environmental life cycle assessment and structural design optimization in engineering practice is essential to contribute to this process.

In this paper, two case studies of hybrid truss structures are described combining environmental life cycle assessment (E-LCC) and life cycle cost assessment (LCC) into a structural multi-objective optimization problem to analyze the E-LCC - LCC trade-off by using a Pareto-efficiency approach. The first case study consists of a simple statically determinate structure, while the second case study is a more complex statically indeterminate structure. For each case study, three design scenarios are investigated: an indoor situation, an outdoor situation, and a fire resistance scenario. Three types of sections can be used and are adapted to the scenario and its specific demands: a timber section, a tubular steel section and a steel tie-rod section.

For the cases considered, the presented approach succeeds in finding a set of Pareto optimal (hybrid) structures. This Pareto front allows the designer to select the structural configuration with the least environmental impact within the budgetary limitations. In addition, it gives an idea of the trade-off between environmental impact and financial cost (how much extra do we have to invest for a certain reduction of the environmental impact). As such, the proposed method can be a useful tool for practicing engineers focusing on sustainable design of structures.

Our study is not free of limitations: first, in order to keep the optimization problem size feasible, the amount of possible configurations was reduced using member section groups. We expected that the Pareto optimal designs would be very similar if this limitation would be lifted, yet it is important to state that in our study the full design space was not utilized. Second, it was found that modelling gaps regarding the toxicity indicators have a substantial impact on the total environmental life cycle cost of a structure. However, when the optimizations are run ignoring the toxicity indicators, the resulting Pareto optimal designs remain very similar.

The results show that hybrid steel/timber designs can be Pareto optimal or even optimal for a single-objective function (E-LCC or LCC). This shows that design rationalization based on intuition and standard practice can lead to sub-optimal results. A multi-objective optimization approach, by contrast, enables the designer to choose the right design based on the design conditions but also on the available resources, as demonstrated by the different sets of Pareto optimal structures for different design scenarios. Nonetheless, it is clear that the ratio of timber and steel elements is a good indicator for the location of a structure in the E-LCC - LCC spectrum (more timber: lower E-LCC, higher LCC; more steel: higher E-LCC, lower LCC). This is however only a useful rule of thumb when deciding for the main material of the structural system and not for the actual configuration of the hybrid structure. Furthermore, the results show that in each case every intermediate Pareto optimal design is a hybrid steel/timber structure. This again stresses the relevance and the usefulness of the presented methodology, as in practice an LCC budget constraint will occur in most cases. This implies that when a designer is oriented towards sustainable construction, but limited by the available financial resources, the optimal design will always be a hybrid steel/timber structure.

CRedit authorship contribution statement

D. Van Cauteren: Writing - original draft, Visualization, Software, Methodology, Formal analysis, Validation, Investigation. **D. Ramon:** Writing - original draft, Visualization, Software, Methodology, Formal analysis, Validation, Investigation. **J. Stroeckx:** Writing - original draft, Conceptualization, Software, Methodology, Investigation, Data curation. **K. Allacker:** Writing - review & editing, Methodology, Supervision, Resources. **M. Schevenels:** Writing - review & editing, Methodology, Supervision, Resources.

Declaration of Competing Interest

The authors declare that they have no known competing financial interests or personal relationships that could have appeared to influence the work reported in this paper.

Acknowledgements

We want to thank B-architecten for their feedback regarding our results for the case based on the Mundo-A building. The work presented in this paper was partly funded by the Research Council of KU Leuven (project C16/17/008). The second author is a PhD fellow of the Research Foundation – Flanders (FWO, grant 1S97418N). The financial support is gratefully acknowledged.

Appendix A. Life cycle inventory

Data regarding the LCI are available as [supplementary material](#).

Appendix B. Life cycle assessment diagrams

The figures in this appendix show supplemental clarifying diagrams regarding the environmental life cycle cost assessment and the financial life cycle cost assessment (see [Figs. B.1–B.6](#)).

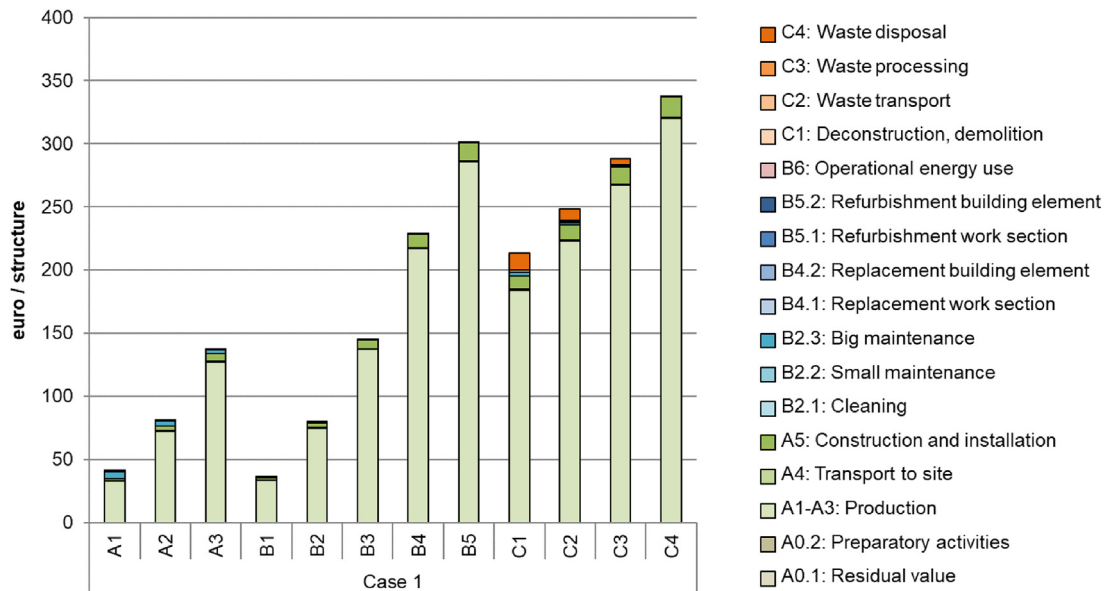


Fig. B.1. Environmental costs for the different Pareto optimal structures grouped per life cycle phase for Case 1.

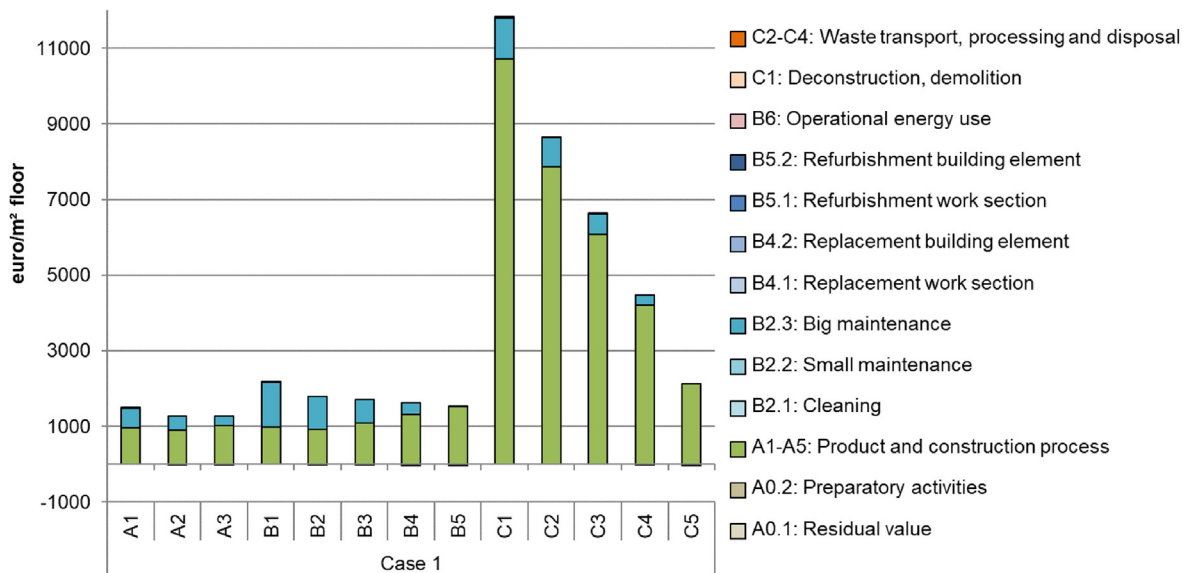


Fig. B.2. Financial costs for the different Pareto optimal structures grouped per life cycle phase for Case 1.

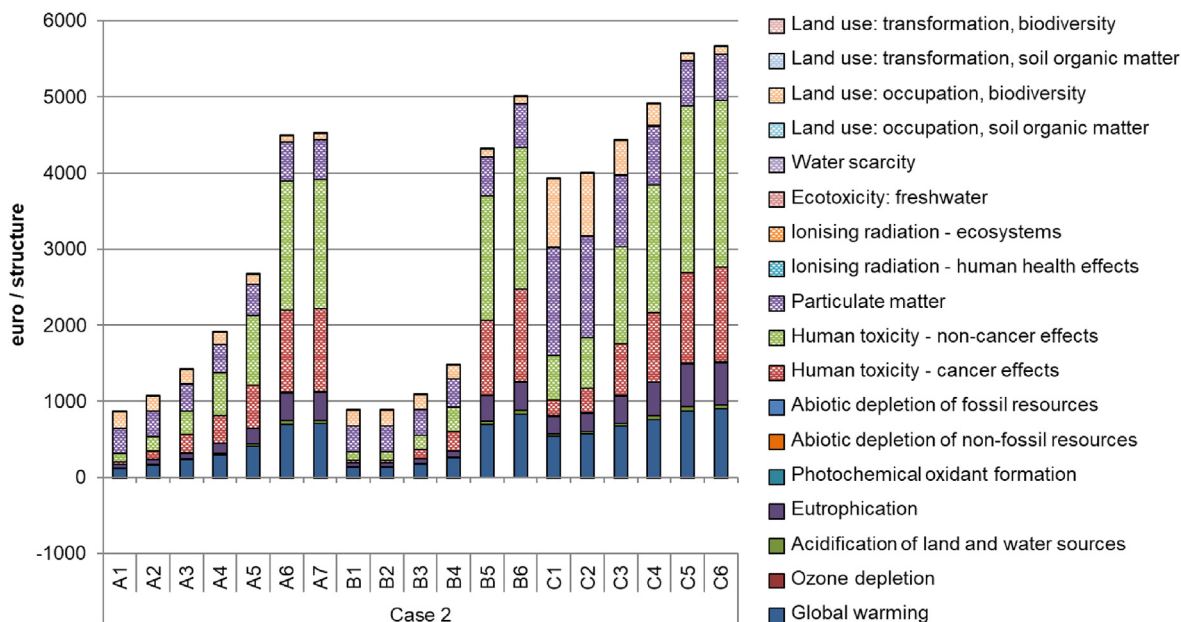


Fig. B.3. Environmental cost for the different Pareto optimal structures grouped per indicator for Case 2.

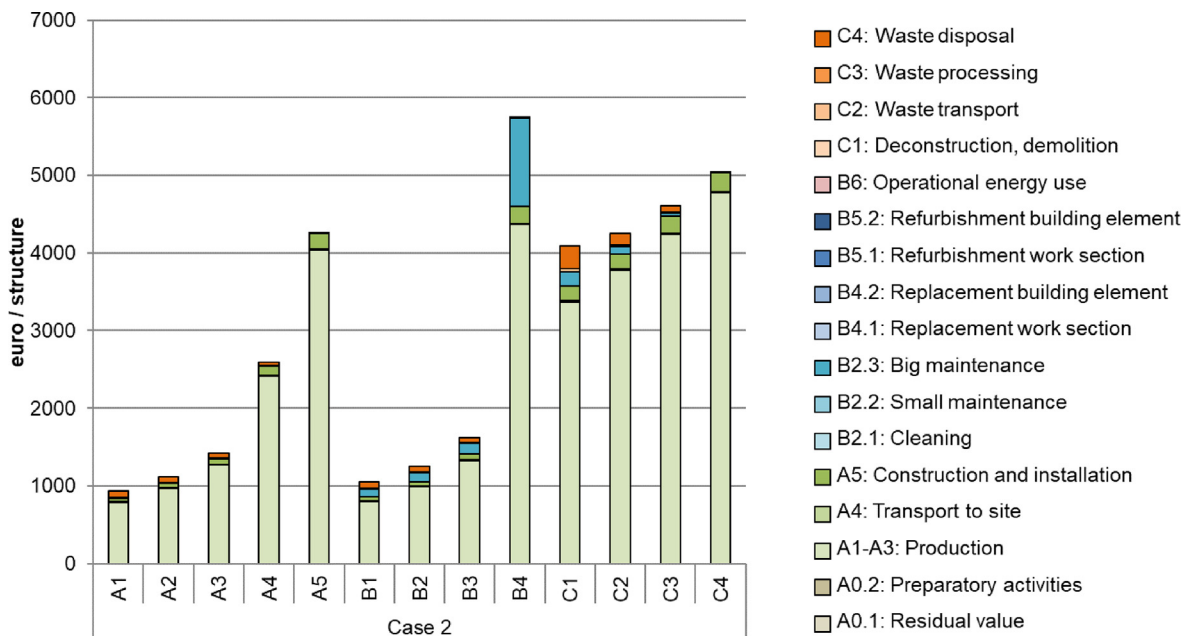


Fig. B.4. Environmental costs for the different Pareto optimal structures grouped per life cycle phase for Case 2.

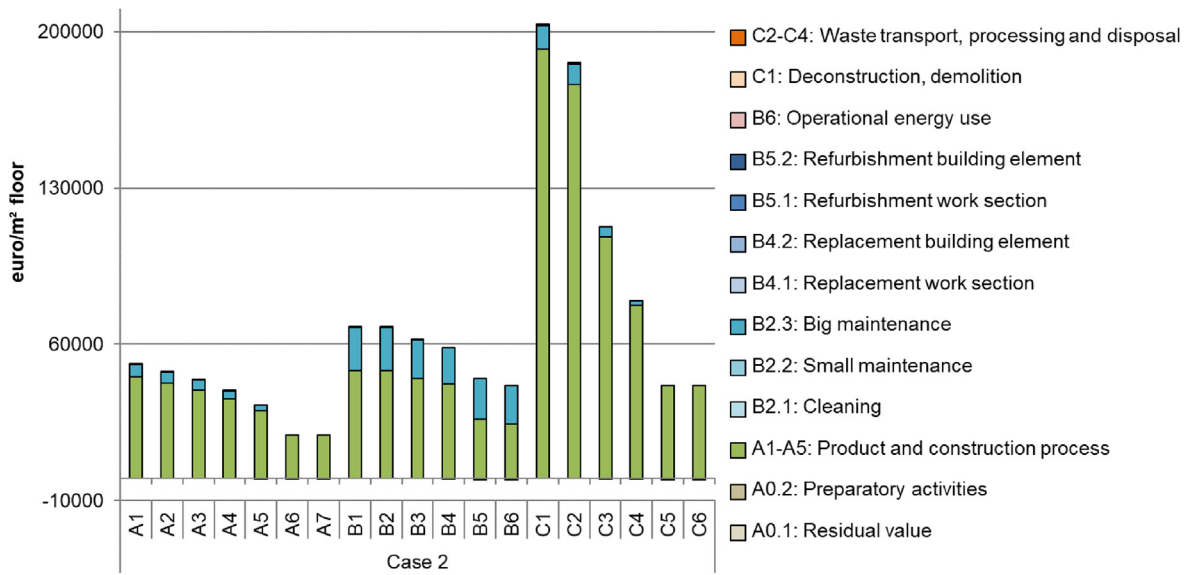


Fig. B.5. Financial costs for the different Pareto optimal structures grouped per life cycle phase for Case 2.

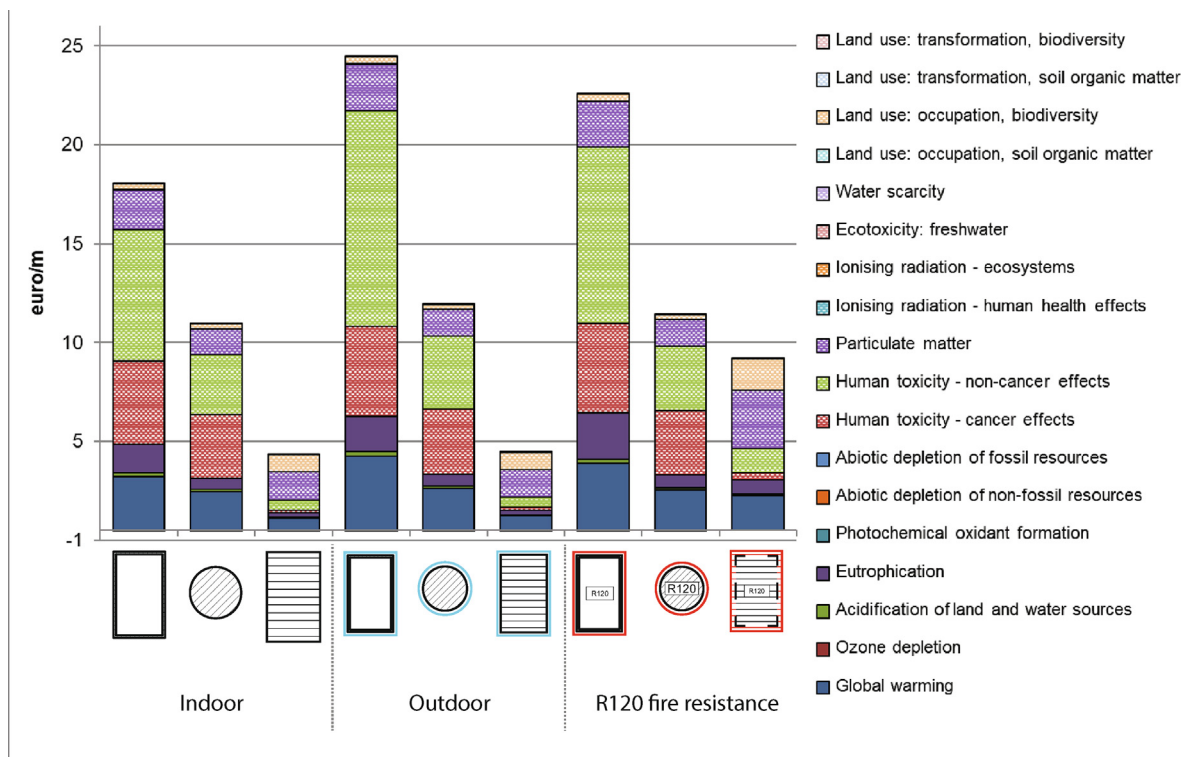


Fig. B.6. Environmental cost for the different type of sections used in Case 2.

Appendix C. Supplementary data

Supplementary data associated with this article can be found, in the online version, at <https://doi.org/10.1016/j.enbuild.2021.111600>.

References

[1] AECOM, editor, Spon's Architects and Builders Price Book 2015, CRC Press, 2015..

[2] AECOM, editor, Spon's Civil Engineering and Highway Works Price Book 2015, CRC Press, 2015..

[3] J. Alcalá, F. González-Vidosa, J.V. Yepes, V. Martí. Embodied energy optimization of prestressed concrete slab bridge decks., *Technologies* 6 (2) (2018) 43..

[4] K. Allacker, Sustainable building. The development of an evaluation method, PhD thesis, KU Leuven, 2010..

[5] K. Allacker, F. De Troyer, D. Trigaux, T. Geerken, C. Spirinckx, W. Debacker, J. Van Dessel, A. Janssen, L. Delem, K. Putzeys, Sustainability, Financial and Quality evaluation of Dwelling Types - SuFiQuaD- final report, 2011..

[6] K. Allacker, W. Debacker, F. De Troyer, A. Janssen, L. Delem, K. Peeters, L. De Nocker, C. Spirinckx, J. Van Dessel, Monetisation of the MMG method (update 2020), 2020..

- [7] Arch-Index, Waarden i-index. <https://www.arch-index.be/indexen/waarden-i>; Accessed: 22-03-2021..
- [8] Hout Info Bios, Afmetingen van hout, 2020. <https://houtinfobois.be/nl/technische-informatie/de-materialen/afmetingen-van-hout/>; Accessed: 06-02-2020..
- [9] N.C. Brown, C.T. Mueller, Design for structural and energy performance of long span buildings using geometric multi-objective optimization, *Energy and Buildings* 127 (2016) 748–761.
- [10] J. Brütting, G. Senatore, C. Fivet, Optimization formulations for the design of low embodied energy structures made from reused elements, in: *Advanced Computing Strategies for Engineering*, Springer International Publishing, 2018, pp. 139–163.
- [11] J. Brütting, C. Vandervaeren, G. Senatore, N. De Temmerman, C. Fivet, Environmental impact minimization of reticular structures made of reused and new elements through life cycle assessment and mixed-integer linear programming, *Energy and Buildings* 215 (2020) 10982..
- [12] M. Conci, T. Konstantinou, A. van den Dobbelsteen, J. Schneider, Trade-off between the economic and environmental impact of different decarbonisation strategies for residential buildings, *Building and Environment* 155 (2019) 137–144.
- [13] L. De Nocker, W. Debacker, Annex: Monetisation fo the MMG method (update 2017), 2018..
- [14] EC-JRC, International Reference Life Cycle Data System (ILCD) Handbook - Recommendations based on existing environmental impact assessment models and factors for Life Cycle Assessment in a European context, 2011..
- [15] CEN (ed), EN 15978 Sustainability of construction works – Assessment of environmental performance of buildings – Calculation method, 2011..
- [16] CEN (ed), EN 15804:2012+A1 Sustainability of construction works – Environmental product declaration – Core rules for the product category of construction products, 2013..
- [17] CEN (ed), EN 16627 Sustainability of construction works – Assessment of economic performance of buildings – Calculation method, 2015..
- [18] S. Eleftheriadis, P. Duffour, D. Mumovic, BIM-embedded life cycle carbon assessment of RC buildings using optimised structural design alternatives, *Energy and Buildings* 173 (2018) 587–600.
- [19] R. Evins, S. Conrad Joyce, P. Pointer, S. Sharma, R. Vaidyanathan, C. Williams, Multi-objective design optimisation: Getting more for less, *Proceedings of the Institution of Civil Engineers - Civil Engineering* 165 (5) (2012) 5–10..
- [20] S. François, M. Schevenels, D. Dooms, M. Jansen, J. Wambacq, G. Lombaert, G. Degrande, G. De Roeck, Stabil: An educational Matlab toolbox for static and dynamic structural analysis, *Computer Applications in Engineering Education* (2021).
- [21] N. Huberman, D. Pearlmutter, E. Gal, I.A. Meir, Optimizing structural roof form for life-cycle energy efficiency, *Energy and Buildings* 104 (2015) 336–349.
- [22] ISO, ISO 14040: Environmental management - Life Cycle Assessment - Principles and Framework, 2006..
- [23] ISO, ISO 14044: Environmental management - Life Cycle Assessment - Requirements and guidelines, 2006..
- [24] ISO, ISO 15686-1: Buildings and constructed assets - Life cycle assessment - Requirements and guidelines, 2006..
- [25] D. Mavrokapnidis, C.C. Mitropoulou, N.D. Lagaros, Environmental assessment of cost optimized structural systems in tall buildings, *Journal of Building Engineering* 24 (2019) 100730.
- [26] K. Mela, Mixed variable formulations for truss topology optimization, PhD thesis, Tampere University of Technology, 2013..
- [27] K. Mela, T. Tiainen, M. Heinisuo, Comparative study of multiple criteria decision making methods for building design, *Advanced Engineering Informatics* 26 (4) (2012) 716–726.
- [28] K. Mela, T. Tiainen, M. Heinisuo, 12.17: Economical design of high strength steel trusses using multi-criteria optimization, *Proceedings of Eurosteel 1 (2–3)* (2017, 2017,) 3613–3621.
- [29] C. Min-Yuan, T. Duc-Hoc, Opposition-based multiple-objective differential evolution to solve the time-cost-environment impact trade-off problem in construction projects, *Journal of Computing in Civil Engineering* 29 (5) (2015).
- [30] Arcelor Mittal, Balkprofielen, 2020..
- [31] M. Najjar, K. Figueiredo, A. Hammad, A. Haddad, Integrated optimization with building information modeling and life cycle assessment for generating energy efficient buildings, *Applied Energy* 250 (2019) 1366–1382.
- [32] M. Nordborg, R. Arvidsson, G. Finnveden, C. Cederberg, L. Sörme, V. Palm, K. Stamy, S. Molander, Updated indicators of swedish national human toxicity and ecotoxicity footprints using USEtox 2.01, *Environmental Impact Assessment Review* 62 (2017) 110–114.
- [33] J. Orr, A. Bras, T. Ibell, Effectiveness of design codes for life cycle energy optimisation, *Energy and Buildings* 140 (2017) 61–67.
- [34] OVAM, Monetisation of the MMG method, 2017..
- [35] M. Röck, M.R.M. Saade, M. Balouktsi, F.N. Rasmussen, H. Birgisdottir, R. Frischknecht, G. Habert, T. Lützkendorf, A. Passer, Embodied GHG emissions of buildings—the hidden challenge for effective climate change mitigation, *Applied Energy* 258 (2020) 114107.
- [36] R. Rosenbaum, T. Bachmann, L. Gold, M. Huijbregts, O. Jolliet, R. Juraske, A. Koehler, H. Larsen, M. MacLeod, M. Margni, et al., USEtox—the UNEP-SETAC toxicity model: recommended characterisation factors for human toxicity and freshwater ecotoxicity in life cycle impact assessment, *The International Journal of Life Cycle Assessment* 13 (7) (2008) 532–546.
- [37] E. Saouter, F. Biganzoli, L. Ceriani, D. Versteeg, E. Crenna, L. Zampori, S. Sala, R. Pant, Environmental footprint: Update of life cycle impact assessment methods—ecotoxicity freshwater, human toxicity cancer, and non-cancer, European Union, Luxembourg, 2018.
- [38] K. Sarma, H. Adeli, Life-cycle cost optimization of steel structures, *International Journal for Numerical Methods in Engineering* 55 (12) (2002) 1451–1462.
- [39] K. Svanberg, The method of moving asymptotes - a new method for structural optimization, *International Journal for Numerical Methods in Engineering* 24 (2) (1987) 359–373.
- [40] K. Svanberg, MMA and GCMMA - two methods for nonlinear optimization, 2007..
- [41] T. Tiainen, M. Laasonen, M. Heinisuo, K. Mela, M. Salminen, T. Jokinen, Multi-criteria optimization of buildings, *Proceedings of the METNET Seminar*, page 72, 2012..
- [42] D. Trigaux, Elaboration of a sustainability assessment method for neighbourhoods, PhD thesis, KU Leuven, 2017..
- [43] OVAM Vandenbroecke, M. Rapport - technische levensduur van gebouwcomponenten, 2018..
- [44] W. Wang, R. Zmeureanu, H. Rivard, Applying multi-objective genetic algorithms in green building design optimization, *Building and Environment* 40 (11) (2005) 1512–1525.
- [45] M.D. Webster, H. Meryman, A. Slivers, T. Rodriguez-Nikl, L. Lemay, K. Simonen, H. Trivedi, L. MacLise, D. Kestner, K. Bland, et al., Structure and carbon-how materials affect the climate, SEI Sustainability Committee, Carbon Working Group, 2012.
- [46] G. Wernet, C. Bauer, B. Steubing, J. Reinhard, E. Moreno-Ruiz, B. Weidema, The ecoinvent database version 3 (part I): overview and methodology, *The International Journal of Life Cycle Assessment* 21 (9) (2016) 1218–1230.
- [47] W.T.C.B. Brandveiligheid, van details en aansluitingen in gebouwen, 2015.
- [48] D.H. Yeo, R.D. Gabbai, Sustainable design of reinforced concrete structures through embodied energy optimization, *Energy and Buildings* 43 (8) (2011) 2028–2033.